Cellular Imaging Hot Paper

DOI: 10.1002/ange.201410645

Ratiometric Fluorescence Imaging of Cellular Polarity: Decrease in Mitochondrial Polarity in Cancer Cells**

Na Jiang, Jiangli Fan, Feng Xu, Xiaojun Peng, Huiying Mu, Jingyun Wang, and Xiaoqing Xiong*

Abstract: *Mitochondrial polarity strongly influences the intracellular transportation of proteins and interactions between biomacromolecules. The first fluorescent probe capable of the ratiometric imaging of mitochondrial polarity is reported. The probe, termed BOB, has two absorption maxima (λ_{abs} = 426 and 561 nm) and two emission maxima—a strong green emission (λ_{em} = 467 nm) and a weak red emission (642 nm in methanol)—when excited at 405 nm. However, only the green emission is markedly sensitive to polarity changes, thus providing a ratiometric fluorescence response with a good linear relationship in both extensive and narrow ranges of solution polarity. BOB possesses high specificity to mitochondria (R_r = 0.96) that is independent of the mitochondrial membrane potential. The mitochondrial polarity in cancer cells was found to be lower than that of normal cells by ratiometric fluorescence imaging with BOB. The difference in mitochondrial polarity might be used to distinguish cancer cells from normal cells.*

Polarity is an important parameter in chemistry and chemical technology.[1] Certain organic or inorganic processes are markedly dependent on the surrounding polarities, which greatly control the reaction processes.[2] In biological systems, especially at the cellular level, polarity determines the interaction activity of a large number of proteins and enzymes or reflects the permeability of membrane compartments. Furthermore, abnormal changes in polarity are closely linked with disorders and diseases (e.g., diabetes, liver cirrhosis).[3] However, polarity is a complex factor and encompasses a range of noncovalent interactions, including dipolarity/polarizability and hydrogen bonding.[4] Thus, its measurement in live cells is difficult and necessitates the development of new tools. Not surprisingly, local polarity differs considerably from one region to another. To better indicate local changes in cells, the sensing of intracellular polarity (as well as other environmental parameters, such as viscosity, and important chemical species, such as Ca^{2+} and singlet oxygen) should to the greatest possible extent be performed within distinct organelles rather than in an unknown intracellular area.[5]

Mitochondria, the principal energy-producing compartments in most cells, function in numerous vital cellular processes, such as ATP production, central metabolism, calcium modulation and redox signaling, and the apoptotic process of cell death.[6,7] Mitochondrial polarity strongly influences the intracellular transportation of proteins and interactions between biomacromolecules. Furthermore, polarity reflects the status and function of this kind of organelle, whose location, morphology, and components are always changing. Several features, such as mitochondrial enzymes, proteins, and macromolecular substances, will not be transmitted in cases of mitochondrial dysfunction.[8] For example, the activity and stability of mitochondrial malate dehydrogenases (mMDHs), important enzymes in numerous mitochondrial proteins, are strongly affected by the amphiphilic microenvironment.[9]

Fluorescent sensors have recently received considerable attention owing to their high sensitivity, selectivity, and nondestructive characteristics.[10] Thus, polarity-sensitive fluorescent probes are considered ideal candidates for sensing polarity in cell biology. Several research teams have developed a number of polarity-sensitive probes based on intramolecular-charge-transfer (ICT) systems[11] to detect local polarity around various proteins, sense the hydrophobic cavities of numerous native proteins, and study the hydrophobic domains of biological macromolecules. Although a few of them are cell-permeable,[12a,b] there are no probes that show specific subcellular organelle distributions and that the activity of a protein or enzyme might be influenced by the local polarity. To date, the detection of mitochondrial polarity in living cells remains a "blank space", with no attempt reported.

Herein, we describe the development of the probe BOB (Figure 1 a), the first mitochondrial molecular probe of polarity, which functions by the ICT mechanism.[13] On the basis of the donor–π-bridge–acceptor (D–π–A) design philosophy, we selected coumarin as the D group because of its high quantum yields, high extinction coefficients, and the fact that this moiety has been engineered to respond to environmental polarity (solvatochromic probes).[14] Concerning the A group, our choice fell on the benzothiazene group owing to its electron-withdrawing aromatic system, which is also capable of extending electron conjugation. Furthermore, the quaternized aromatic amino groups impart good water solubility to

[*] N. Jiang, J. Fan, F. Xu, Prof. X. Peng, H. Mu, X. Xiong
State Key Laboratory of Fine Chemicals
Dalian University of Technology
2 Linggong Road, 116024 Dalian (China)
E-mail: fanjl@dlut.edu.cn
Prof. J. Wang
School of Life Science and Biotechnology
Dalian University of Technology
2 Linggong Road, 116024 Dalian (China)

[**] This research was financially supported by the NSF of China (21136002, 21376039, 21422601, and 21421005), the National Basic Research Program of China (2013CB733702), the Ministry of Education (NCET-12-0080), Liaoning NSF (2013020115), and Fundamental Research Funds for the Central Universities (DUT14ZD214).

Supporting information for this article is available on the WWW under http://dx.doi.org/10.1002/anie.201410645.

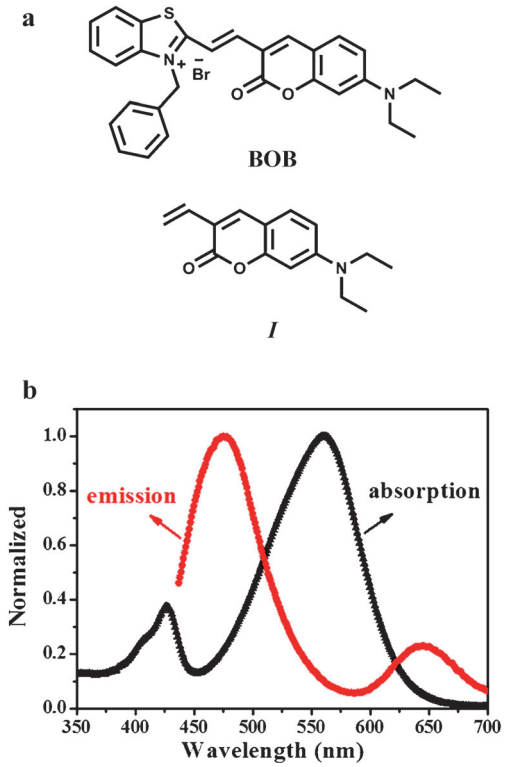

Figure 1. a) Molecular structures of BOB and **I**. b) Normalized absorption and emission spectra (excitation at 405 nm) of BOB in methanol.

the probe, and the benzyl group helps the probe to accumulate in mitochondria.[15] BOB has a linear ratiometric fluorescence response to solution polarity and is the first fluorescent probe to image mitochondrial polarity. We found for the first time that the mitochondrial polarity in cancer cells tends to be lower than that of normal cells. The difference in polarity could be discriminated to a remarkable extent by ratiometric fluorescence imaging.

BOB has two absorption maxima ($\lambda_{abs} = 426$ nm, $\varepsilon = 1.00 \times 10^4\ mol^{-1}\,cm^{-1}\,L$ and $\lambda_{abs} = 561$ nm, $\varepsilon = 2.6 \times 10^4\ mol^{-1}\,cm^{-1}\,L$) and two emission maxima ($\lambda_{em} = 467$ and 642 nm, excitation at 405 nm) in methanol (Figure 1b; see also Table S1 in the Supporting Information). To identify which part of the molecule was responsible for the short-wavelength emission of BOB, we studied the absorption and emission properties of three parts of the molecule (see Figure S1 in the Supporting Information) by DFT calculations in methanol. The absorption and fluorescence emission of **I** (Figure 1a) occur 424 and 488 nm, respectively (see Figure S2), which are very close to the wavelengths of BOB in methanol ($\lambda_{abs,test} = 426$ nm and $\lambda_{em,test} = 467$ nm). The calculated absorption and emission wavelengths of BOB ($\lambda_{abs} = 560$ nm and $\lambda_{em} = 645$ nm) are in complete accord with the test results. Therefore, we deduced that the red emission is due to the extended π-conjugation as well as strong ICT from the diethylaminocoumarin moiety (represented by **I**) to the conjugated hemicyanine moiety, whereas the emission band at 467 nm can probably be ascribed to part **I**.

The absorption and fluorescence spectra of BOB were then measured at 25 °C in a variety of solvents covering a large polarity range, as expressed by the orientation polarizability. The Lippert–Mataga polarity parameter Δf is related to solvent orientational polarization.[16] Only tiny changes were discernible in the absorption maxima in all of these solvents with different polarity (see Figure S3). In contrast, solvent polarity had a dramatic effect on the emission spectra, in which solvatochromic behavior usually originates from large variations in the molecular dipole upon photon absorption, thus leading to different stabilization energies of the ground and excited states as a result of the solvent shell around the molecule. When the solvent polarity increases, this effect becomes more significant: The excited state releases more energy to reach a more stable state, thus resulting in low fluorescence intensity or/and a shift in the absorption/fluorescence spectrum.[17] Furthermore, the larger dipole moments of the excited state lead to a larger solvating effect.[18] In our case, as the dipole moment of **I** in different solvents is larger than that of BOB (see Table S3), the green emission is more markedly sensitive to solution polarity changes than the red emission upon the excitation of BOB at 405 nm. When the polarity (Δf) of the solution was decreased from 0.32 (water) to 0.013 (toluene), the fluorescence intensity of BOB at 467 nm increased by a factor of 24, and the red emission at 645 nm gave a slight fluorescence response (see Figure S4 and Table S2), thus providing a ratiometric response. Thus, a linear relationship exists between the fluorescence intensity (I_{467}/I_{645}) and Δf, which demonstrated

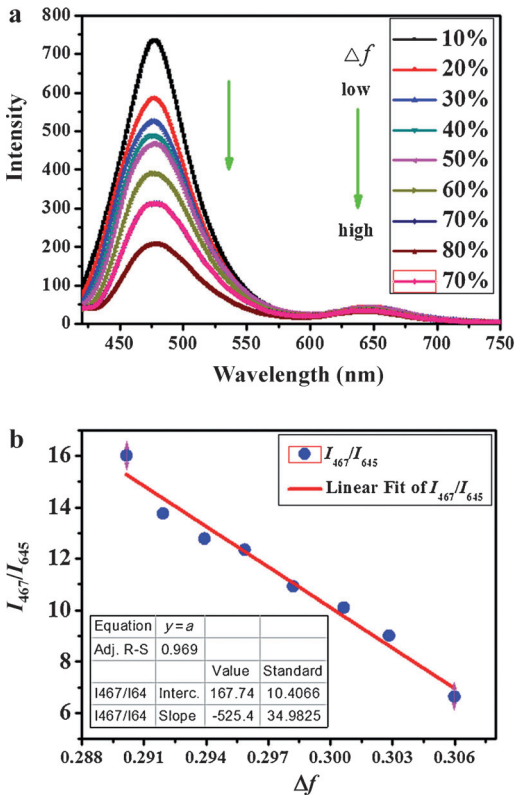

Figure 2. a) Fluorescence emission spectra in water/1,4-dioxane solvent mixtures (the percentage in the box indicates the water content). b) Linearity of I_{467}/I_{645} versus the solvent parameter Δf (with excitation in all cases at 405 nm).

that BOB could be employed to ratiometrically detect extensive solution polarity.

In a narrow polarity range with different proportions of water and 1,4-dioxane, the same result was observed for the absorption maxima as during extensive solution polarity (see Figure S5). In contrast, when the polarity (Δf) of the solution decreased from 0.31 (80% water) to 0.29 (10% water), the fluorescence intensity of BOB at 467 nm was increased by a factor of 3.5, whereas the red emission at 645 nm showed only a slight response in the form of a slight fluorescence enhancement (from 31.4 to 45.8; Figure 2). This finding also shows a good linear correlation of the fluorescence intensity I_{467}/I_{645} with Δf, which demonstrates that BOB is highly sensitive to solvent polarity and can potentially reveal the polarity of its immediate environment.

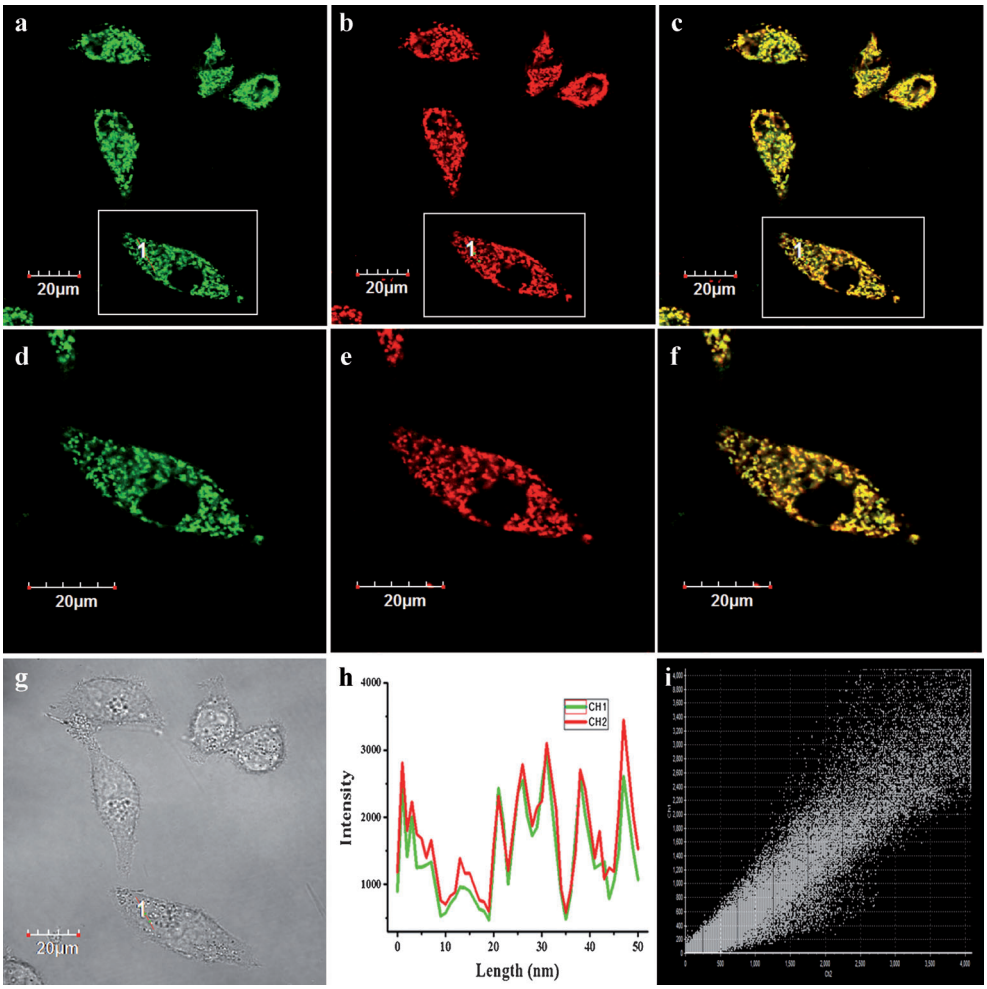

Figure 3. a, b) Confocal fluorescence images of MCF-7 cells stained with Mito Tracker Green FM (2.0 μM) for 15 min (a) and BOB (2.0 μM) for 15 min (b). c) Merged image of (a) and (b). d–f) Enlarged representations of cells in image (a), (b), and (c), respectively. g) Bright-field image. h) Intensity profile of regions of interest (ROIs) across MCF-7 cells. i) Correlation plot of the intensities of Mito Tracker Green FM and BOB ($R_r = 0.96$).

To assess the photophysical behavior of the prepared coumarin–hemicyanine hybrids in a biological environment, we examined compound BOB in living cells. Confocal fluorescence microscopy showed that MCF-7 cells labeled with BOB emitted fluorescence with maximal wavelengths of 468 and 645 nm (see Figure S6). The wavelengths were nearly identical to those observed for BOB in the extracellular environment. Collected images showed that the probe was emissive in subcellular compartments, which were sometimes filamentous or slightly swollen (see Figures S6 and S7). On morphological grounds, the compartments were judged to be mitochondria.[19] Hydrophilicity–lipophilicity was modeled by the logarithm of the water–octanol partition coefficient ($\log P$). Probes specifying mitochondrial accumulation were numerically assigned on the basis of the following criteria: electric charge $Z > 0$ and $0 < \log P < +5$.[20] For BOB, the Z_{BOB} and $\log P_{BOB}$ values were 1 and 2.8, respectively, which indicate that BOB can probably be trapped in mitochondria. To further investigate the subcellular localization of BOB, a commercially available, mitochondria-localizing dye, MitoTracker Green FM, was used for a colocalization study in two types of cell lines, MCF-7 cells (Figure 3) and HepG2 cells (see Figure S8). Colocalization was quantified by the use of Pearson sample correlation factors (R_r). The intensity of the correlation plots revealed a high R_r value of 0.96. We also performed the BOB colocalization experiments with the commercial lysosome fluorescent dye LysoTracker Green DND (see Figure S9) and the endoplasmic reticulum fluorescent dye ER-Tracker Green (see Figure S10). No colocalization was observed in these two cases. All results confirmed that BOB was a true mitochondrion-targeted probe.[21]

We examined BOB staining in MCF-7 cells treated with the membrane-potential uncoupler 3-chlorophenylhydrazone (CCCP), which can disrupt the mitochondrial membrane potential.[22] Both the green and the red channel of confocal fluorescence images were unchanged in the absence or presence of CCCP (see Figure S11), thus suggesting that BOB was independent of the mitochondrial membrane potential. Given that cell toxicity is a key feature for live-cell imaging, the cytotoxicity of BOB was then evaluated in an MTT assay. The dye showed low cell cytotoxicity at low (2.0 μM, cell viability $\geq 96\%$) and high concentrations

(10.0 μM, cell viability ≥86%; see Figure S12). All results showed that BOB was poorly cytotoxic to living cells under our cell-imaging conditions. In a pH-titration study, the fluorescence signal of BOB changed very little (see Figure S13), thus indicating that the fluorescence of BOB was not influenced by the pH microenvironment. Photobleaching is a common problem for most organic dyes and often compromises the temporal monitoring of dynamic events inside cells because of the fading of reporter dyes.[11h,23] Upon irradiation for 10 h with a 500 W iodine–tungsten lamp, the density of BOB remained at 89%, but that of MitoTracker Deep Red FM (commercial) decreased to less than 65% (see Figure S14). These results indicate the high photostability of BOB under environmental conditions. Furthermore, the fluorescence in both green and red channels did not decrease significantly upon discontinuous laser irradiation for 30 min (see Figure S15).

During the experiment, we found that mitochondrial polarity varied as the cell status changed (Figure 4). In terms of their morphology, the RAW 264.7 cells usually display an irregular spindle shape or visible longer pseudopodia, so the cells in area 1 were in the normal state. As the cells approach death, they become circular, as in area 2. In Figure 4d, the green region represents higher polarity ($\Delta f = 0.297$), and the color amaranth stands for lower polarity ($\Delta f = 0.284$). Thus, we deduce that mitochondrial polarity in dying cells is lower than that in normal cells. To verify this phenomenon, we used the drug etoposide to induce apoptosis. We found that during apoptosis, the amaranth-colored areas increased in size, and the size of the green region decreased (see Figure S16c–f), which means that mitochondrial polarity was reduced.

The activity of mMDH in cirrhosis patients is higher than that in a healthy person, and mMDH shows relatively high activity in low-polarity microenvironments.[24] Therefore, we inferred that mitochondrial polarity in cirrhosis patients is lower than in healthy persons. Thus, two types of normal cells (cos-7 and RAW 264.7 cells) and three kinds of cancer cells (HeLa, HepG2, and MCF-7 cells) were selected to be incubated with BOB. After the cells were incubated with BOB (2.0 μM) for 15 min, green- and red-channel confocal images were collected. The green area in the two types of normal cells was larger than that in the three types of cancer cells, which indicated that the mitochondrial polarity in both cos-7 and RAW 264.7 ($\Delta f = 0.295$) was higher than in HeLa ($\Delta f = 0.288$), HepG2 ($\Delta f = 0.290$), and MCF-7 cells ($\Delta f = 0.287$; Figure 5).

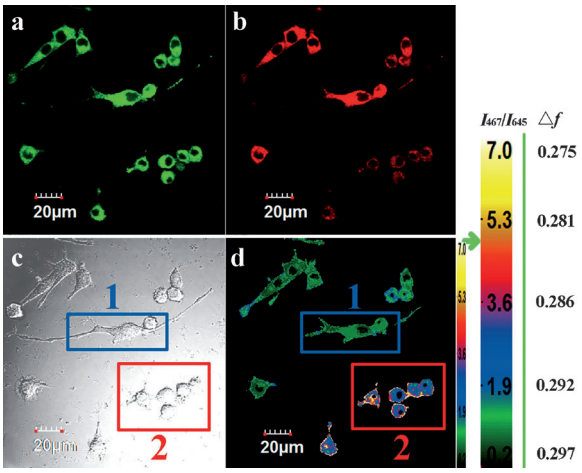

Figure 4. a, b) Confocal fluorescence images of RAW 264.7 cells. Images were acquired by using excitation and emission windows of $\lambda_{ex} = 405$ nm, $\lambda_{em} = 435$–535 nm (a) and $\lambda_{ex} = 405$ nm, $\lambda_{em} = 575$–675 nm (b). c) Bright-field images of cells. d) Fluorescence ratio images.

In conclusion, we have developed the probe BOB, the first fluorescent probe for mitochondrial polarity, on the basis of a coumarin–hemicyanine dye. Significantly, BOB has a linear ratiometric fluorescence response to both extensive and narrow ranges of solution polarity. Furthermore, BOB localizes in mitochondria and is independent of mitochondrial membrane potential, thus making it suitable as an indicator of polarity changes in the mitochondrial microenvironment. Mitochondrial polarity data for cos-7 cells, RAW 264.7 cells, HeLa cells, HepG2 cells, and MCF-7 cells were obtained.

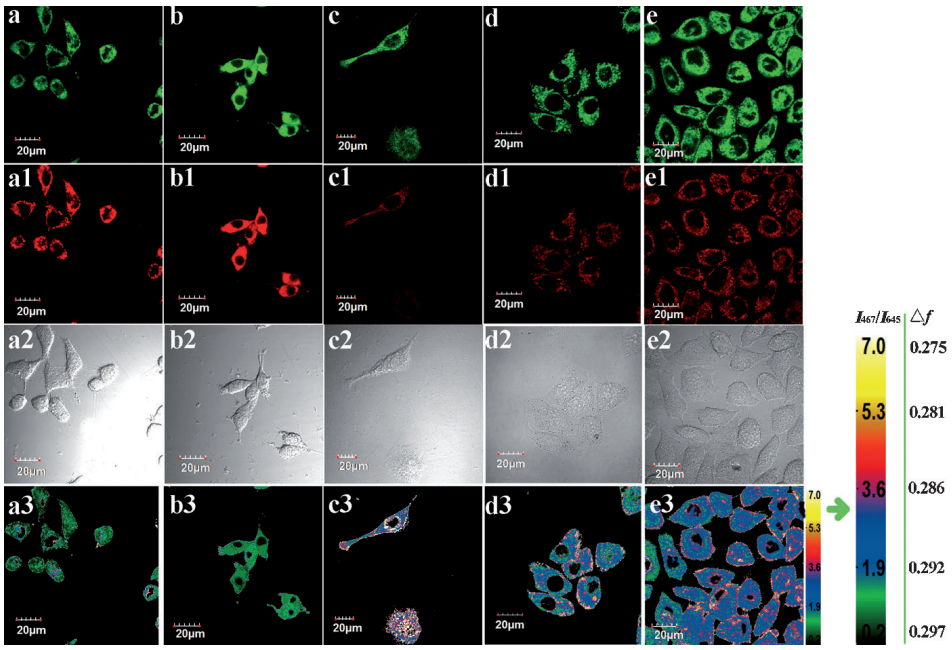

Figure 5. Imaging of a–a3) cos-7 cells, b–b3) RAW 264.7 cells, c–c3) HeLa cells, d–d3) HepG2 cells, and e–e3) MCF-7 cells. a–e and a1–e1) Confocal fluorescence images with $\lambda_{em} = 435$–535 nm for (a–e) and $\lambda_{em} = 575$–675 nm for (a1–e1). a2–e2) Bright-field images of the cells. a3–e3) Fluorescence ratio images.

Differences in polarity could be discriminated to a remarkable extent by ratiometric fluorescence imaging. Furthermore, we found that mitochondrial polarity in cancer cells tends to be lower than in normal cells. We hope that the detection of mitochondrial polarity can be used as a new method in the future to distinguish cancer cells from normal cells. Further research is under way.

Received: October 31, 2014
Published online: January 8, 2015

Keywords: cancer sensing · dyes · mitochondria · polarity · ratiometric imaging

[1] S. Ercelen, A. S. Klymchenko, A. P. Demchenko, *Anal. Chim. Acta* **2002**, *464*, 273 – 287.
[2] Z. G. Yang, J. F. Cao, Y. X. He, J. H. Yang, T. Kim, X. J. Peng, J. S. Kim, *Chem. Soc. Rev.* **2014**, *43*, 4563 – 4601.
[3] a) Y. D. Zhuang, P. Y. Chiang, C. W. Wang, K. T. Tan, *Angew. Chem. Int. Ed.* **2013**, *52*, 8124 – 8128; *Angew. Chem.* **2013**, *125*, 8282 – 8286; b) M. W. Berns, T. Krasieva, C. H. Sun, A. Dvornikov, P. M. Rentzepis, *J. Photochem. Photobiol. B* **2004**, *19*, 51 – 56; c) L. Huang, S. W. Tam-Chang, *J. Fluoresc.* **2011**, *21*, 213 – 222.
[4] a) B. Szczupak, A. G. Ryder, D. M. Togashi, A. S. Klymchenko, Y. A. Rochev, A. Gorelov, T. J. Glynn, *J. Fluoresc.* **2010**, *20*, 719 – 731; b) P. Suppan, *J. Chem. Soc. A* **1968**, 3125 – 3133.
[5] a) L. Wang, Y. Xiao, W. M. Tian, L. Z. Deng, *J. Am. Chem. Soc.* **2013**, *135*, 2903 – 2906; b) M. K. Kuimova, S. W. Botchway, A. W. Parker, M. Balaz, H. A. Collins, H. L. Anderson, K. Suhling, P. R. Ogilby, *Nat. Chem.* **2009**, *1*, 69 – 73; c) Y. Koide, Y. Urano, S. Kenmoku, H. Kojima, T. Nagano, *J. Am. Chem. Soc.* **2007**, *129*, 10324 – 10325; d) S. Chalmers, S. T. Caldwell, C. Quin, T. A. Prime, A. M. James, A. G. Cairns, M. P. Murphy, J. G. McCarron, R. C. Hartley, *J. Am. Chem. Soc.* **2012**, *134*, 758 – 761.
[6] a) H. Rottenberg, *Biochemistry* **1992**, *31*, 9473 – 9481; b) G. L. Martin, C. Lau, S. D. Minteer, M. J. Cooney, *Analyst* **2010**, *135*, 1131 – 1137; c) C. W. T. Leung, Y. Hong, S. Chen, E. Zhao, J. W. Y. Lam, B. Z. Tang, *J. Am. Chem. Soc.* **2013**, *135*, 4926 – 4929.
[7] a) P. H. Reddy, M. F. Beal, *Brain Res. Rev.* **2005**, *49*, 618 – 632; b) H. M. McBride, M. Neuspiel, S. Wasiak, *Curr. Biol.* **2006**, *16*, 551 – 560; c) J. Estaquier, D. Arnoult, *Cell Death Differ.* **2007**, *14*, 1086 – 1094.
[8] a) D. Wang, J. Wang, G. M. C. Bonamy, S. Meeusen, R. G. Brusch, C. Turk, P. Yang, P. G. Schultz, *Angew. Chem. Int. Ed.* **2012**, *51*, 9302 – 9305; *Angew. Chem.* **2012**, *124*, 9436 – 9439; b) T. Landes, J. C. Martinou, *Biochim. Biophys. Acta Mol. Cell Res.* **2011**, *1813*, 540 – 545; c) L. F. Yousif, K. M. Stewart, S. O. Kelley, *ChemBioChem* **2009**, *10*, 1939 – 1950.
[9] a) R. A. Musrati, M. Kollarova, N. Mernik, D. Mikulasova, *Gen. Physiol. Biophys.* **1998**, *17*, 193 – 210; b) J. W. Callahan, G. W. Kosicki, *Can. J. Biochem.* **1967**, *45*, 839 – 850.
[10] Y. Zhou, J. F. Zhang, J. Yoon, *Chem. Rev.* **2014**, *114*, 5511 – 5571.
[11] a) G. Saroja, T. Soujanya, B. Ramachandram, A. Samanta, *J. Fluoresc.* **1998**, *8*, 405 – 410; b) H. Sauer, L. Pratsch, R. Peters, *Anal. Biochem.* **1991**, *194*, 418 – 424; c) K. Kudo, A. Momotake, J. K. Tanaka, Y. Miwa, T. Arai, *Photochem. Photobiol. Sci.* **2012**, *11*, 674 – 678; d) H. Sunahara, Y. Urano, H. Kojima, T. Nagano, *J. Am. Chem. Soc.* **2007**, *129*, 5597 – 5604; e) O. A. Kucherak, S. Oncul, Z. Darwich, D. A. Yushchenko, Y. Arntz, P. Didier, Y. Mély, A. S. Klymchenko, *J. Am. Chem. Soc.* **2010**, *132*, 4907 – 4916; f) G. Loving, B. Imperiali, *J. Am. Chem. Soc.* **2008**, *130*, 13630 – 13638; g) C. Huang, Q. Yin, W. Zhu, Y. Yang, X. Wang, X. Qian, Y. Xu, *Angew. Chem. Int. Ed.* **2011**, *50*, 7551 – 7556; *Angew. Chem.* **2011**, *123*, 7693 – 7698; h) F. Amin, D. A. Yushchenko, J. M. Montenegro, W. J. Parak, *ChemPhysChem* **2012**, *13*, 1030 – 1035.
[12] a) A. Toutchkine, V. Kraynov, K. Hahn, *J. Am. Chem. Soc.* **2003**, *125*, 4132 – 4145; b) G. Signore, R. Nifosì, L. Albertazzi, B. Storti, R. Bizzarri, *J. Am. Chem. Soc.* **2010**, *132*, 1276 – 1288.
[13] a) J. Massin, A. Charaf-Eddin, F. Appaix, Y. Bretonnière, D. Jacquemin, B. Sanden, C. Monnereau, C. Andraud, *Chem. Sci.* **2013**, *4*, 2833 – 2843; b) S. Giovanni, N. Riccardo, A. Lorenzo, B. Ranieri, *J. Biomed. Nanotechnol.* **2009**, *5*, 722 – 729; c) M. Koenig, G. Bottari, G. Brancato, V. Barone, D. M. Guldi, T. Torres, *Chem. Sci.* **2013**, *4*, 2502 – 2511.
[14] a) H. Turki, S. Abid, S. Fery-Forgues, R. E. Gharbi, *Dyes Pigm.* **2007**, *73*, 311 – 316; b) T. Hirano, K. Hiromoto, H. Kagechika, *Org. Lett.* **2007**, *9*, 1315 – 1318.
[15] a) "One-class bi-benzyl pentamethyl cyanine fluorescent dye, and preparation method and application thereof": J. Fan, L. A. Lee, X. Peng, X. Qiang, Q. Wang, China Patent. WO2013075285A1, **2013**; b) M. H. Lee, N. Park, C. Yi, J. H. Han, J. H. Hong, K. P. Kim, D. H. Kang, J. L. Sessler, C. Kang, J. S. Kim, *J. Am. Chem. Soc.* **2014**, *136*, 8430 – 8437.
[16] a) W. Qin, M. Baruah, M. Sliwa, M. V. D. Auweraer, W. M. D. Borggraeve, D. Beljonne, B. V. Averbeke, N. Boens, *J. Phys. Chem. A* **2008**, *112*, 6104 – 6114; b) A. Niemann, A. Takatsuki, H. P. Elsässer, *J. Histochem. Cytochem.* **2000**, *48*, 251 – 258; c) R. C. Weast, *Handbook of Chemistry and Physics*, CRC, Boca Raton, FL, **1980**.
[17] J. R. Lakowicz, *Principles of Fluorescence Spectroscopy*, Springer, 3rd ed., **2010**.
[18] a) L. Ding, Z. Zhang, X. Li, J. Su, *Chem. Commun.* **2013**, *49*, 7319 – 7321; b) L. Yang, X. Li, J. B. Yang, Y. Qu, J. L. Hua, *ACS Appl. Mater. Interfaces* **2013**, *5*, 1317 – 1326.
[19] J. S. Lee, Y. K. Kim, M. Vendrell, Y. T. Chang, *Mol. BioSyst.* **2009**, *5*, 411 – 421.
[20] a) F. Rashid, R. W. Horobin, *Histochemistry.* **1990**, *94*, 303 – 308; b) R. W. Horobin, J. C. Stockert, F. Rashid-Doubell, *Histochem. Cell Biol.* **2006**, *126*, 165 – 175.
[21] a) M. H. Lee, J. H. Han, J. H. Lee, H. G. Choi, C. Kang, J. S. Kim, *J. Am. Chem. Soc.* **2012**, *134*, 17314 – 17319; b) K. Sreenath, J. R. Allen, M. W. Davidson, L. Zhu, *Chem. Commun.* **2011**, *47*, 11730 – 11732.
[22] a) A. Harriman, L. J. Mallon, G. Ulrich, R. Ziessel, *ChemPhysChem* **2007**, *8*, 1207 – 1214; b) C. S. Russell, Jr., W. G. Lee, *Biophys. J.* **1999**, *76*, 469 – 477.
[23] H. Kobayashi, M. Ogawa, R. Alford, P. L. Choyke, Y. Urano, *Chem. Rev.* **2010**, *110*, 2620 – 2640.
[24] Q. Y. Chen, X. Lv, Z. J. Zhang, H. Dai, *J. Clin. Exp. Med.* **2011**, *10*, 347 – 348.

